The complement membrane attack complex triggers intracellular Ca^{2+} fluxes leading to NLRP3 inflammasome activation

Kathy Triantafilou*, Timothy R. Hughes, Martha Triantafilou and B. Paul Morgan
Institute of Infection and Immunity, School of Medicine, Cardiff University, Heath Park, Cardiff CF14 4XN, UK
*Author for correspondence (TriantafilouK@cardiff.ac.uk)

Accepted 27 March 2013
Journal of Cell Science 126, 2903–2913

doi: 10.1242/jcs.124388

Summary

The membrane attack complex of complement (MAC), apart from its classical role of lysing cells, can also trigger a range of non-lethal effects on cells, acting as a drive to inflammation. In the present study, we chose to investigate these non-lethal effects on inflammasome activation. We found that, following sublytic MAC attack, there is increased cytosolic Ca^{2+} concentration, at least partly through Ca^{2+} release from the endoplasmic reticulum lumen via the inositol 1,4,5-triphosphate receptor (IP_3R) and ryanodine receptor (RyR) channels. This increase in intracellular Ca^{2+} concentration leads to Ca^{2+} accumulation in the mitochondrial matrix via the 'mitochondrial calcium uniporter' (MCU), and loss of mitochondrial transmembrane potential, triggering NLRP3 inflammasome activation and IL-1β release. NLRP3 co-localises with the mitochondria, probably sensing the increase in calcium and the resultant mitochondrial dysfunction, leading to caspase activation and apoptosis. This is the first study that links non-lethal effects of sublytic MAC attack with inflammasome activation and provides a mechanism by which sublytic MAC can drive inflammation and apoptosis.

Key words: Complement membrane attack complex, Inflammasome, NLRP3, IL-1β

Introduction

The innate immune system is one of the most ancient cornerstones of immunity acting as a rapid and efficient immune surveillance system that constantly monitors the extracellular and intracellular compartments for signs of infection and tissue damage leading to inflammation. Key components of the innate immune sensing apparatus include the complement system, which acts as a first line of defence against microbial pathogens, recognising and quickly tagging and eliminating the pathogens; the pattern recognition receptors (PRRs) such as the Toll-like receptors (TLRs), the NOD-like receptors (NLRs) and RIG-like receptors (RLRs) that detect pathogen-associated molecular patterns (PAMPs) and trigger pro-inflammatory responses; and finally a cytosolic surveillance system termed the inflammasome, which forms large multimolecular complexes that control caspase-1 activation and IL-1β secretion.

Although initially thought to be separate sensor entities constituting linear cascades of separate sensor pathways, it is now emerging that all the components of the innate immune system operate as a hub-like network that is tightly controlled (Hajishengallis and Lambris, 2010; Hajishengallis and Lambris, 2011). There is increasing evidence for extensive and bi-directional cooperation between the different sensors shaping the inflammatory response. Depending on the trigger, there are several initiation and regulatory mechanisms that act together to produce an anticipated result in immune surveillance: for example, triggering of TLRs and RLRs acts as a priming step for the inflammasome (Rathinam et al., 2012), while synergic and antagonistic crosstalk occurs between TLRs and complement (Hawlisch et al., 2005; Zhang et al., 2007; Fang et al., 2009; Wang et al., 2010). The question that remains is whether there is crosstalk between the inflammasome and complement.

Mechanisms by which complement activates cells include the binding of activated complement fragments to their receptors and effects induced by sublytic attack by terminal components C5b-9. The membrane attack complex (MAC), formed by the self-polymerization of terminal components of the complement cascade, binds to the surfaces of target cells and effects cytolysis by forming transmembrane pores or channels in the cell membrane (Mayer, 1972; Bhakdi and Tranum Jensen, 1991). It is possible that by forming transmembrane pores in the membrane, complement transmits a danger signal from the extracellular space inside the cell triggering inflammation. In this study, we investigated whether these MAC pores trigger inflammasome activation in the cytosol, since membrane permeability and channel formation on the cell membrane has been recently shown to trigger inflammasome activation (Ichinohe et al., 2010).

Our investigations revealed that sublytic attack by MAC leads to caspase-1 activation as well as IL-1β secretion, indicative of inflammasome activation. Furthermore, using shRNA, we have implicated NALP3 as the main inflammasome that is being activated. In addition, we reveal that MAC insertion triggers Ca^{2+} influx and increased cytosolic Ca^{2+} concentration, at least partly through Ca^{2+} release from the endoplasmic reticulum lumen via the inositol 1,4,5-triphosphate receptor (IP_3R) and ryanodine receptor (RyR) channels. This increase in intracellular Ca^{2+}

concentration leads to Ca^{2+} accumulation into the mitochondrial matrix via MCU, the "mitochondrial calcium uniporter" (MCU), mitochondrial dysfunction, apoptosis, inflammasome activation and IL-1β secretion. These findings demonstrate a novel link between sublytic MAC attack and inflammasome activation and reveal how MAC can amplify on-going inflammatory responses.

Results

Sublytic MAC formation on epithelial cells

In order to deposit MAC on the surface of lung epithelial cells, cells were grown in monolayers and incubated with a polyclonal rabbit anti-CD59 antiserum to permit complement activation and MAC assembly. CD59 antiserum and increasing amounts of normal human serum (NHS) led to a concentration-dependent increase in cell death as determined by PI staining (Fig. 1A). Sublytic doses of MAC were defined as <5% cell death. MAC assembly was confirmed by flow cytometry and immunofluorescence analysis (Fig. 1B); cells were treated with anti-CD59/NHS at a sublytic dose (5% NHS) (open histogram) or with anti-CD59/heat-inactivated NHS (HI-NHS) at the same dose (grey histogram). Flow cytometry confirmed presence of the MAC through positive staining for C9 neoepitope after sublytic activation of complement (Fig. 1B, open histogram), whereas cells treated with HI-NHS were negative for MAC staining (Fig. 1B, grey histogram).

Sublytic MAC formation activates the inflammasome

In order to determine whether sublytic MAC activation triggers pro-inflammatory cytokine secretion, we investigated the secretion of IL-6 (Fig. 2A) and IL-8 (Fig. 2B). There was cytokine production in response to a combination of anti-CD59 and a sublytic dose of NHS, whereas in the presence of anti-CD59 and HI-NHS, as well as HI-NHS or NHS alone, the production was negligible, demonstrating that cytokine production occurred only in response to sublytic MAC formation.

In order to verify that MAC formation was the trigger of the cytokine production observed, we incubated the cells with anti-CD59 in combination with the same dose of NHS which had been depleted for C5, C7 or C9. It was shown that when serum depleted for any of these terminal complement components was used, there was no significant cytokine production.

In order to investigate whether MAC formation is detected by the inflammasome, we assessed inflammasome activation by measuring IL-1β secretion by ELISA (Fig. 2C) and caspase p10 activation/fragmentation by western blotting (Fig. 2D) from lung epithelial cells. The data demonstrated that sublytic MAC formation resulted in IL-1β secretion (Fig. 2C) as well as caspase-1 activation (Fig. 2D). This was also confirmed using HEK-blue IL-1β reporter cells (Fig. 2E). IL-1β secretion was not observed in response to NHS alone, anti-CD59 plus HI-NHS or anti-CD59 plus NHS depleted for C5, C7 or C9, demonstrating a requirement for MAC assembly in order to trigger inflammasome activation.

Sublytic MAC formation activates the NLRP3 inflammasome

To verify which NLR inflammasome was triggered in response to MAC formation, expression of individual NLRPs were knocked down by shRNA (Fig. 3A) followed by an assessment of IL-1β secretion and caspase 1 activation in response to sublytic MAC formation; the data demonstrated a significant reduction in IL-1β secretion (Fig. 3B) when NLRP3 or the inflammasome adaptor ASC was knocked down while there was no significant change in IL-1β secretion when NLRP1 or NLRC4 were knocked down (Fig. 3B). IL-6 production in response to sublytic MAC

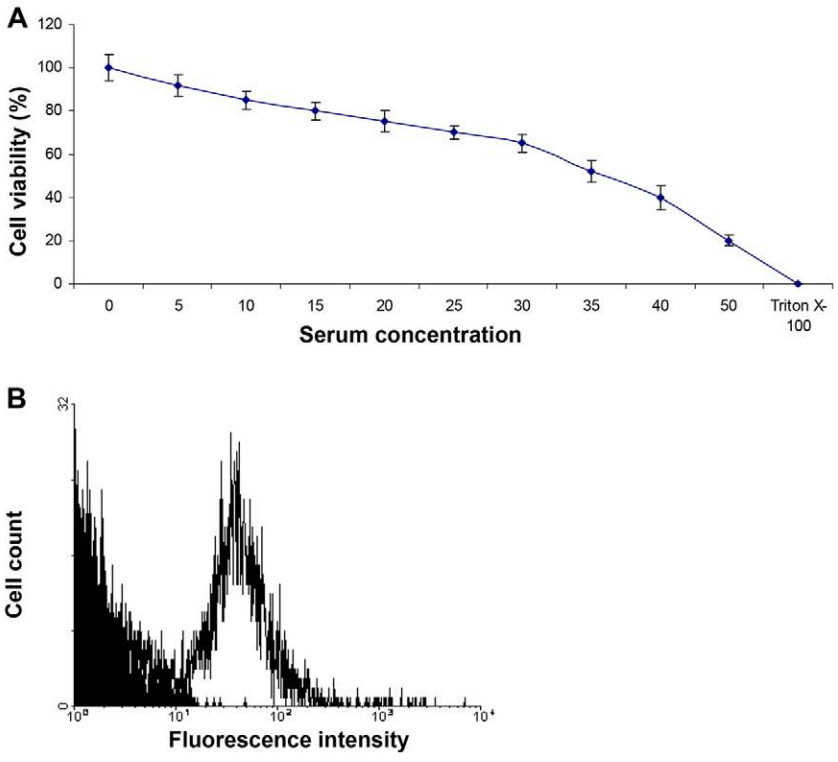

Fig. 1. Titration of sublytic MAC. (**A**) Propidium iodide assay measuring the amount of cell death after treating lung epithelial cells with anti-CD59 as sensitiser, and ascending concentrations of NHS for 1 h at 37℃. For negative controls, cells were treated with anti-CD59/HI-NHS, and for the positive control with 1% Triton X-100. Data are means±s.d. (n=3). (**B**) The level of MAC deposition at different doses of serum was revealed by mean fluorescence intensity upon staining for the anti-C9 neoepitope using flow cytometry in anti-CD59 sensitised cells.

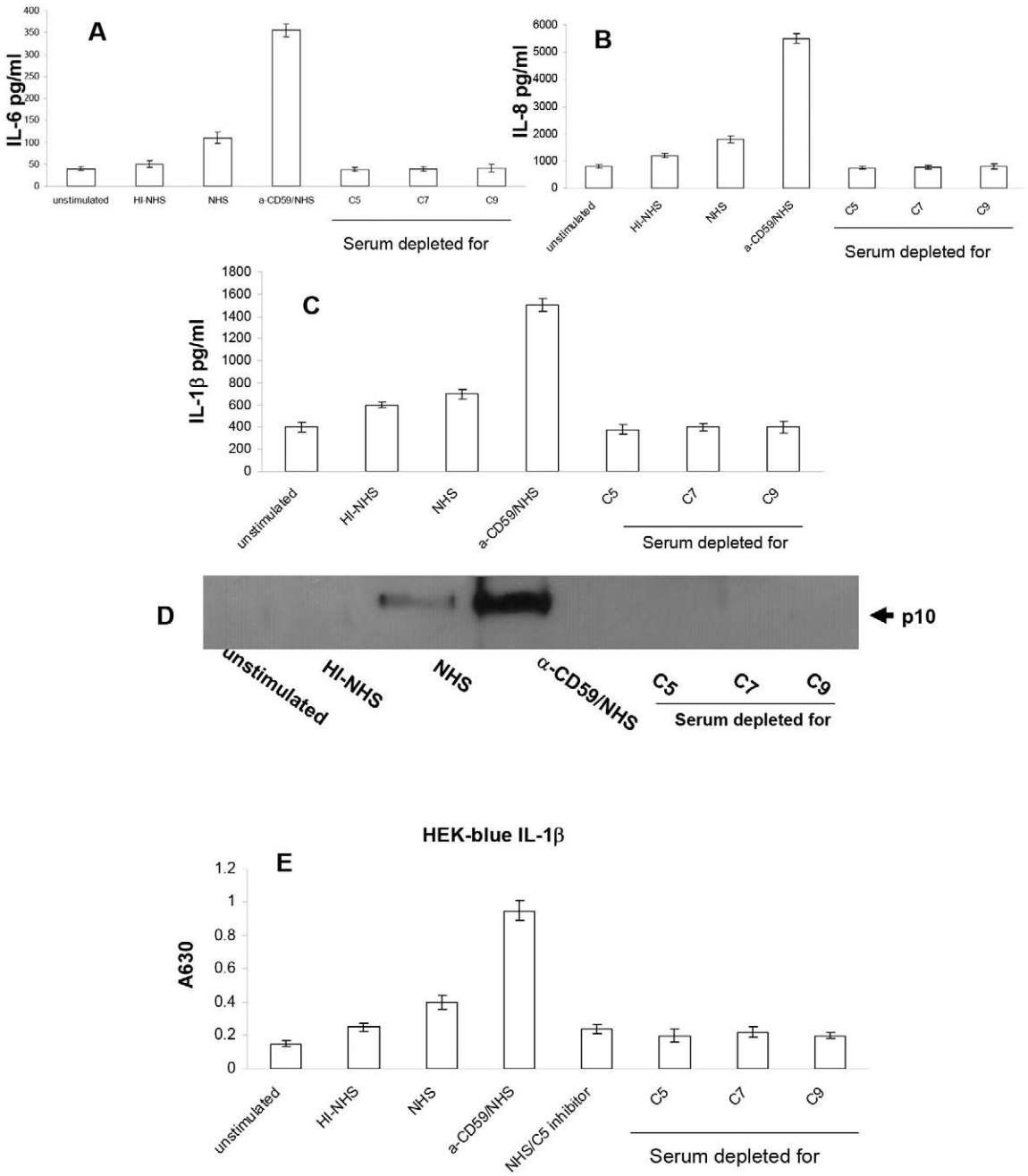

Fig. 2. Cytokine production in response to sublytic MAC. Lung epithelial cells were incubated with either HI-NHS or NHS, or pre-treated with anti CD59 and 5% NHS (in order to provoke, 5% cell death – sublytic MAC), NHS depleted for terminal complement components C5, C7 or C9 (A–D) or NHS containing C5 inhibitor (E). Supernatant was collected at 12 h post incubation and analysed for IL-6 (**A**), IL-8 (**B**) and IL-1β (**C**) using the CBA bead array system on a FACSCalibur (Becton Dickinson). Data are means±s.d. of three independent experiments. (**D**) Cell extracts were analysed for the presence of caspase p10 by western blotting. (**E**) Activation of the inflammasome was confirmed using the HEK-Blue IL-1β reporter cell line.

formation remained unaffected in cells where NLRP1, NLRP3, ASC or NLRC4 were knocked down (Fig. 3C).

In order to verify the activation of NLRP3 in response to MAC, we elucidated the intracellular interactions of the NLRP3 inflammasome, caspase p10 and ASC in the presence of MAC (Fig. 3D) using confocal microscopy.

In order to quantify the degree of co-localisation, we used Costes' approach (Bolte and Cordelières, 2006). This allows for the calculation of Pearson's correlation coefficient R(obs), which also accounts for any random overlay of pixels by generating the mean correlation coefficient R(rand) between n images that have identical average pixel intensity to the original images, but a random distribution of pixels. R(obs) is not sensitive to background and has a linear regression range of −1 to 1, with −1 being total negative correlation, 0 being a random correlation and 1 being total positive. In theory, an R(obs) of +1 would represent a perfect pixel correlation between two channels in an image. Values greater than 0.5 are considered significant co-localisation. In addition, Costes'

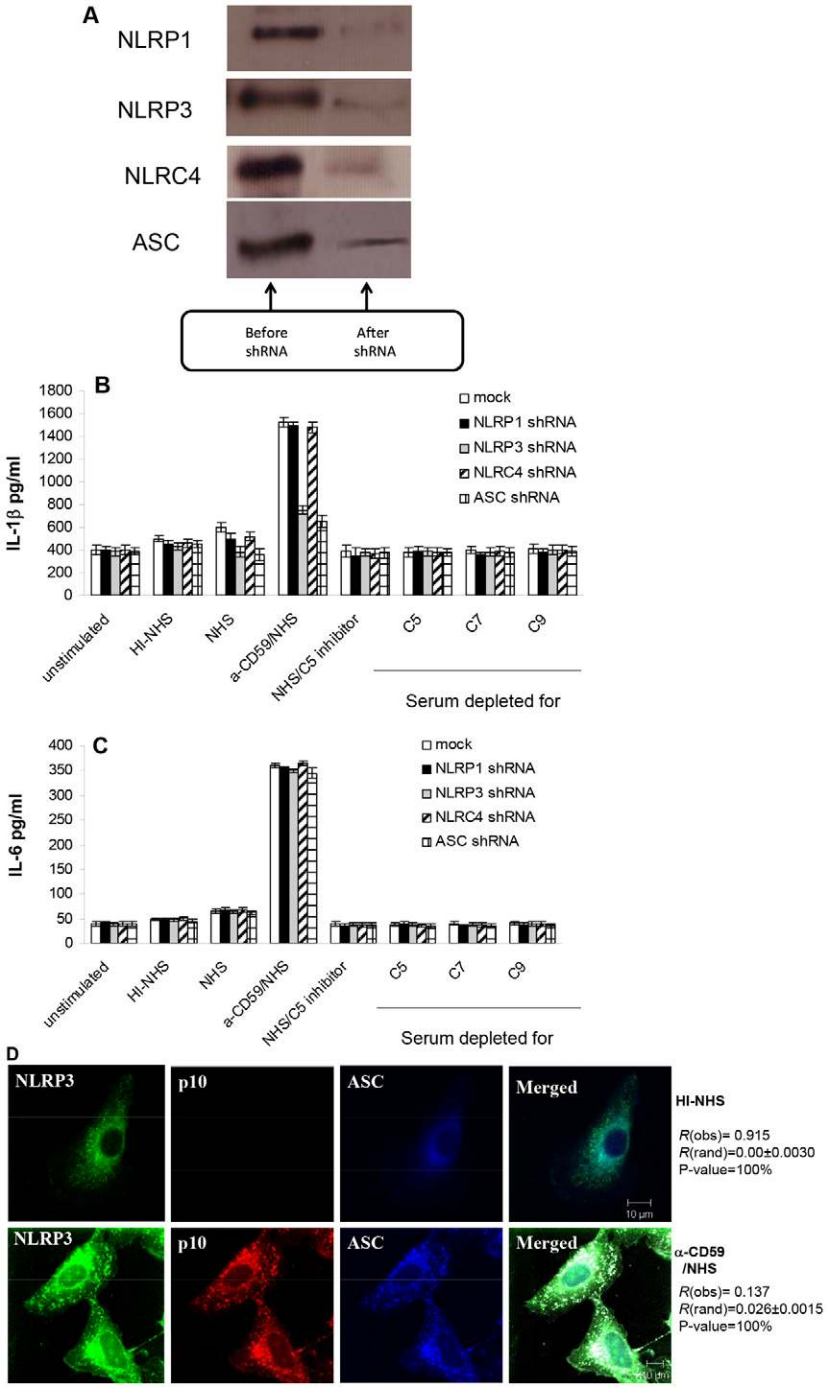

Fig. 3. The NLRP3 inflammasome is triggered in response to sublytic complement. NLRP1, NLRP3 and NLRC4 expression was knocked down by shRNA (**A**) and the cells were again incubated with HI-NHS, NHS, anti-CD59 and 5% NHS (in order to provoke <5% cell death – sublytic MAC), NHS containing C5 inhibitor, or depleted for terminal complement components C5, C7 or C9. Supernatant was collected after 12 h and analysed for IL-1β (**B**) and IL-6 (**C**) using the CBA system. Data are means±s.d. of three independent experiments. (**D**) The localisation of NLRP3, caspase p10 and ASC was investigated when cells were either treated with HI-NHS (top row), or with anti-CD59 and NHS (bottom row). Cells were stimulated with either NI-NHS or anti-CD59 and NHS for 1 h and subsequently fixed. NLRP3 was stained using a rabbit anti NLRP3 Fab conjugated to Alexa 488, caspase p10 was stained using a rabbit polyclonal caspase 1 p10 antibody conjugated to Alexa 543 and ASC was stained using a goat anti-ASC Fab conjugated to Alexa 633. Cells were imaged using a Zeiss 510 confocal microscope. Scale bars: 10 μm. Co-localisation coefficients [*R*(obs)] were calculated using Costes' approach.

randomisation method calculates the statistical significance of the Pearson's correlation coefficient. It returns a significance (*P* value) expressed as a percentage.

It was shown that when cells were treated with anti-CD59 and HI-NHS, there was no caspase p10 expression, suggesting that there was no NLRP3 inflammasome activation (Fig. 3D, top row). In contrast when cells were treated with anti-CD59 and a sublytic dose of NHS, caspase p10 was expressed and appeared to co-localise with NLRP3 and ASC (Fig. 3D, bottom row), a distribution indicative of inflammasome activation. The statistical significance of these observations was confirmed using Costes' approach, which returned an *R*(obs) of 0.915, which is close to the theoretical maximal value therefore suggesting that these co-localisations are highly significant.

Increase in cytosolic Ca^{2+} concentration following MAC formation

It has been previously shown that the first detectable event upon sublytic MAC formation on the cell surface is Ca^{2+} influx and increased cytosolic Ca^{2+} concentration (Morgan and Campbell, 1985; Morgan et al., 1986). It is believed that in nucleated cells the increased intracellular Ca^{2+} concentration stimulates recovery processes, allowing the cell to escape complement membrane attack, but also activating the production of inflammatory

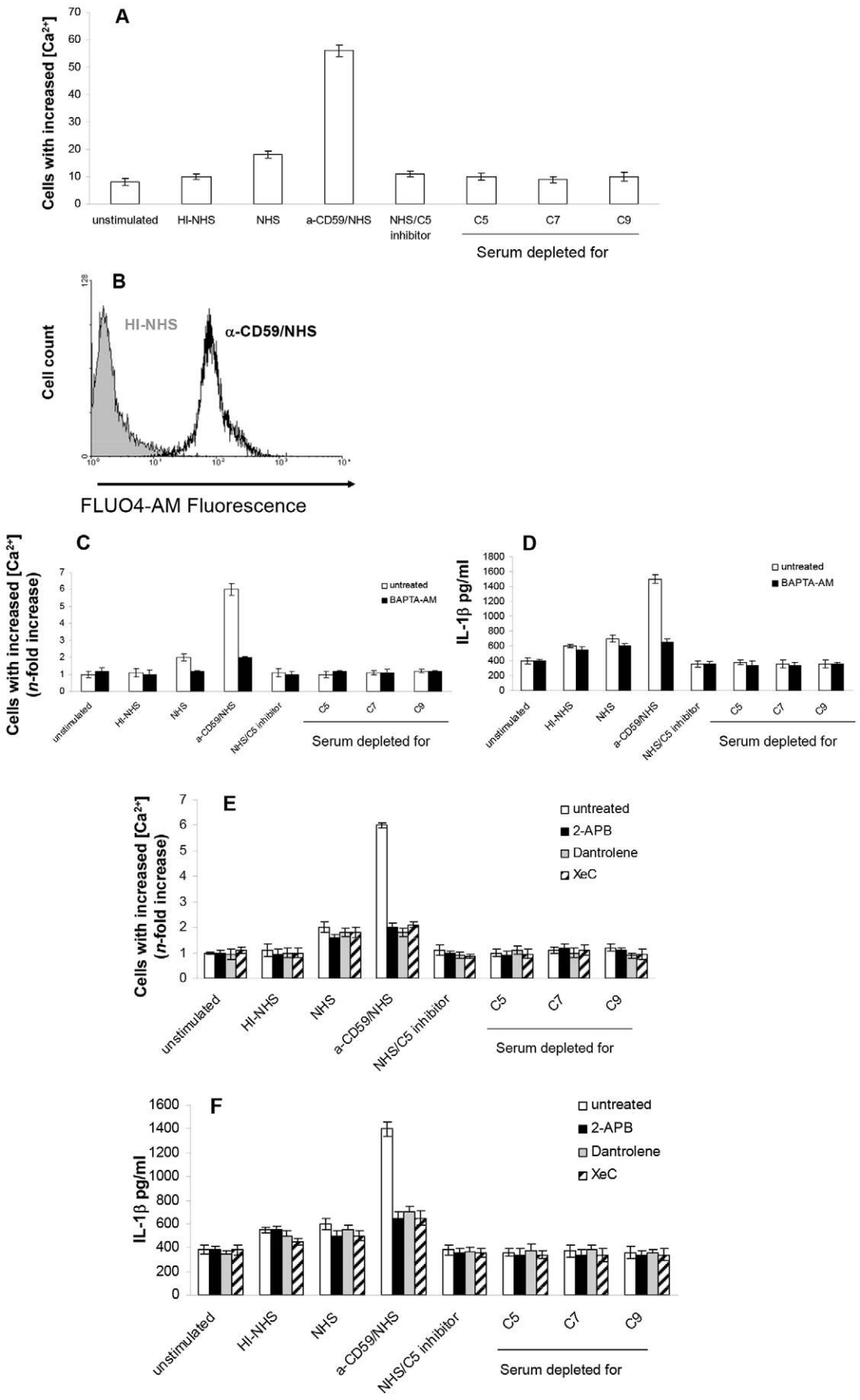

Fig. 4. See next page for legend.

mediators (Morgan et al., 1986). Therefore in this study we proceeded to investigate whether sublytic MAC formation triggered increased cytosolic Ca^{2+} concentration and whether this leads to inflammasome activation.

The Ca^{2+} sensitive dye FLUO4-AM was used to stain cells for the determination of cytosolic Ca^{2+} by flow cytometry. Sublytic MAC formation resulted in a significant increase in cytosolic Ca^{2+} (Fig. 4A), whereas when sensitised cells were either incubated with NHS that was depleted for C5, C7 or C9 or were incubated with HI-NHS (Fig. 4B) there was no Ca^{2+} influx.

To investigate a possible role of cytosolic Ca^{2+} in NLRP3 inflammasome activation we used a permeant Ca^{2+} chelator, 1,2-bis(*o*-aminophenoxy)ethane-*N*,*N*,*N*′,*N*′-tetra-acetic acid tetra(acetoxymethyl) ester (BAPTA-AM). Cells were left untreated or were treated with BAPTA-AM (15 μM) 2 h prior to MAC formation. Entrapped BAPTA decreased the elevation in cytosolic Ca^{2+} concentration in cells which had been challenged by sublytic MAC (Fig. 4C). In addition, BAPTA significantly decreased the secretion of IL-1β induced by sublytic MAC (Fig. 4D), suggesting that Ca^{2+} signalling is crucial for MAC-triggered NLRP3 inflammasome activation.

Sublytic MAC formation induces the release of Ca^{2+} from the ER

Ca^{2+} can be released from intracellular stores, predominantly from the ER through IP_3R and/or RyR channels, such channels have been previously implicated in apoptotic Ca^{2+} signalling between intracellular stores and mitochondria (Celsi et al., 2009; Deniaud et al., 2008). In order to investigate whether the MAC induced increase in cytosolic Ca^{2+} was due in part to release from intracellular stores, via IP_3R and/or RyR channels, cells were treated with inhibitors of IP_3R and/or RyR channels, 2-aminoethoxydiphenyl borate (2-APB) (10 μM), xestospongin C (XeC) (10 μM) and dantrolene (20 μM) respectively. It was shown that all the inhibitors reduced the MAC-triggered increase in cytosolic Ca^{2+} (Fig. 4E), suggesting that there is Ca^{2+} release from the ER lumen through these channels after MAC formation. Most interestingly, the inhibitors reduced IL-1β production in response to MAC formation (Fig. 4F), suggesting that Ca^{2+} release from intracellular stores in the ER lumen is primarily responsible for triggering NLRP3 inflammasome activation.

Ca^{2+} release from the ER is involved in MAC-induced apoptosis

We hypothesised that the Ca^{2+} store release and activation of the NLRP3 inflammasome may reflect the ability of elevated cytosolic Ca^{2+} to trigger mitochondrial damage. We therefore investigated the effect of sublytic MAC on mitochondrial dysfunction, particularly membrane potential ($\Delta\psi_m$), as well as cytochrome *c* efflux into the cytosol. $\Delta\psi_m$ was measured by flow cytometric analysis of cells stained with $DiOC_6$ as well as JC-1 (5,5′,6,6′-tetrachloro1,1′,3,3′-tetramethylbenzimidazolylcarbocyanine iodide) dye. Sublytic MAC formation caused a drop in $\Delta\psi_m$ (Fig. 5A); this was inhibited in cells treated with BAPTA-AM (Fig. 5A), suggesting that the Ca^{2+} release was responsible for the observed drop in $\Delta\psi_m$.

JC-1 dye was also used to monitor mitochondrial potential. JC-1 dye is widely used in studies to monitor mitochondrial health. JC-1 dye exhibits potential-dependent accumulation in mitochondria, indicated by a fluorescence emission shift from green (~529 nm) to red (~590 nm). Consequently, mitochondrial depolarization is indicated by a decrease in the red/green fluorescence intensity ratio. The monomeric form has an emission maximum of ~529 nm. The dye at higher concentrations or potentials forms red fluorescent J-aggregates with an emission maximum at 590 nm (Smiley et al., 1991). Cells treated with JC-1 showed progressive loss of red J-aggregate fluorescence and increase of the green monomer fluorescence following exposure to anti-CD59 and NHS (Fig. 5B, bottom row), whereas when treated with HI-NHS the membrane potential remained unchanged (Fig. 5B, top row), suggesting MAC-induced depolarization of the mitochondrial membrane.

Similar results were obtained with cytochrome *c*. Cytochrome *c* efflux into the cytosolic fraction was analysed by western blotting in cells exposed to sublytic MAC. Cytochrome *c* was detected in the cytoplasm of MAC exposed cells and this was inhibited by pretreatment of cells with BAPTA-AM (Fig. 5C). These data suggest that the increase in cytosolic Ca^{2+} concentration following sublytic MAC formation plays a role in triggering mitochondrial dysfunction and apoptosis.

Ca^{2+} translocation into mitochondria plays a role in MAC-induced apoptosis

Since Ca^{2+} release from the ER contributes to mitochondrial dysfunction, NLRP3 activation and apoptosis in cells exposed to sublytic MAC activation, we proceeded to investigate the mechanisms involved.

Ca^{2+} exchange between the ER and mitochondria can play a key role in apoptosis, therefore Ca^{2+} influx into mitochondria was assessed in cells exposed to MAC formation, using the fluorescent mitochondrial probe Rhod2 AM. Mitochondrial Ca^{2+} uptake was determined by flow cytometry. Our results showed that there was an increase of cells displaying elevated mitochondrial Ca^{2+} (Fig. 6A,B).

In order to investigate the mechanism of mitochondrial Ca^{2+} uptake in response to sublytic MAC deposition, we proceeded to knock down the recently identified mitochondrial calcium uniporter (MCU) (De Stefani et al., 2011; Baughman et al., 2011). Silencing of MCU (Fig. 6C) markedly reduced the mitochondrial Ca^{2+} uptake (Fig. 6D) and consequently IL-1β production (Fig. 6E). Therefore suggesting that MAC-induced Ca^{2+} accumulation into the mitochondrial matrix occurs via MCU. IL-6 secretion was measured as a control for the siRNA effect since it is independent of inflammasome activation but is a known marker for NF-κB activation. As expected, it remained unaffected (Fig. 6F).

Since NLRP3 was shown to be activated in response to the increase in Ca^{2+} concentration following MAC formation, we investigated the localisation of NLRP3 using confocal

Fig. 4. Sublytic MAC-induced increase in cytosolic Ca^{2+} secondary to release from the ER. (**A**) Lung epithelial cells were incubated with HI-NHS, NHS, anti-CD59 and 5% NHS (in order to provoke <5% cell death – sublytic MAC), NHS containing C5 inhibitor, or depleted for terminal complement components C5, C7 or C9, and the calcium-sensitive dye FLUO4-AM was used to measure the cytosolic calcium level by flow cytometry. (**B**) Representative flow cytometry histograms after FLUO-4 staining of cells treated with HI-NHS (grey histogram) or anti-CD59 and NHS (white histogram). Cells were also treated with the intracellular Ca^{2+} chelator BAPTA-AM (**C**,**D**) or IP_3R and RyR channel inhibitors 2-APB (10 μM), dantrolene (20 μM) or XeC (10 μM) (**E**,**F**), and the cytosolic Ca^{2+} concentration (C,E) and IL-1β secretion (D,F) were measured. Data are means±s.d. of three independent experiments.

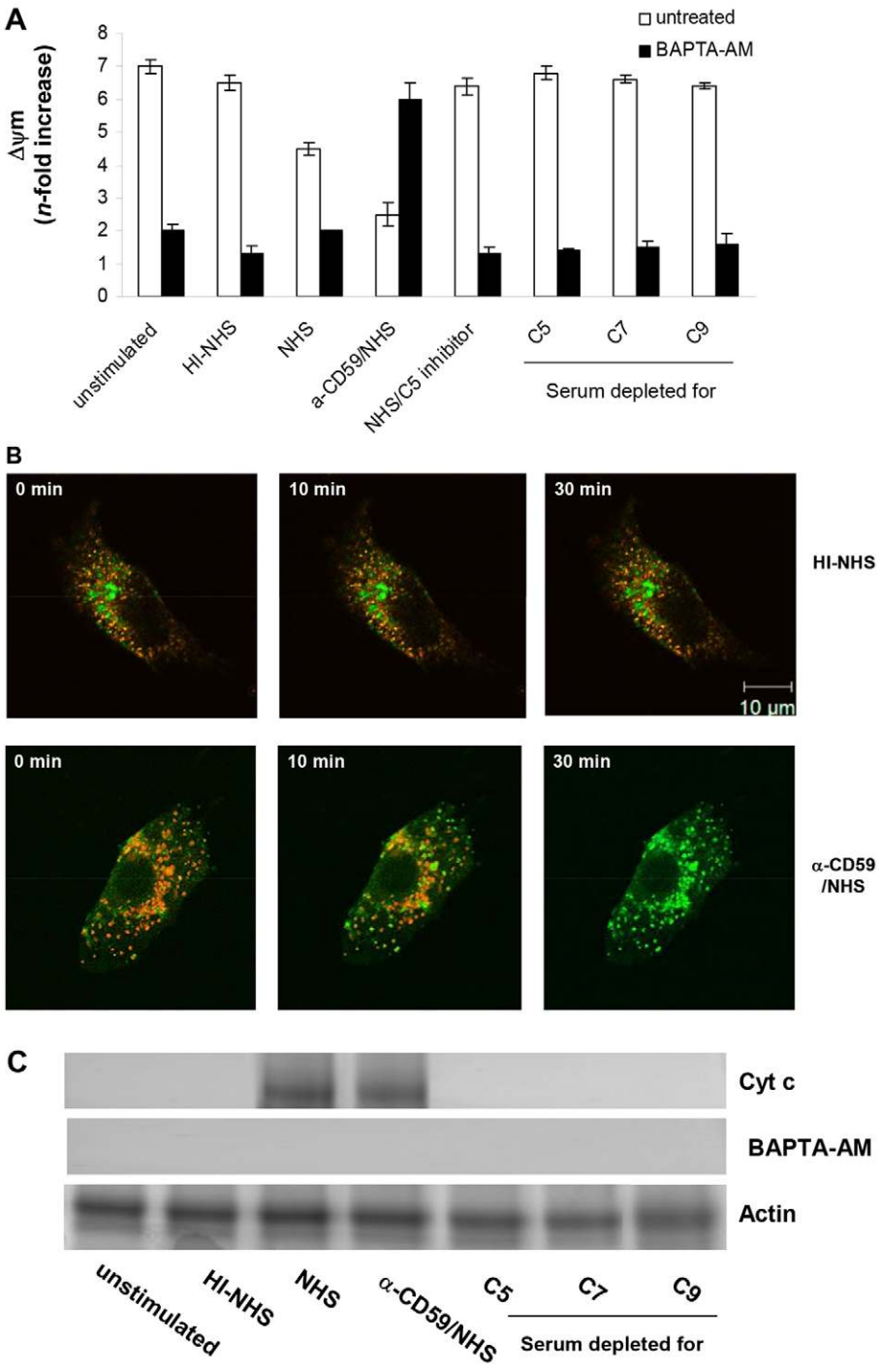

Fig. 5. Sublytic MAC induces mitochondrial dysfunction and cytochrome *c* release. Lung epithelial cells were incubated with HI-NHS, NHS, anti-CD59 and 5% NHS (in order to provoke <5% cell death – sublytic MAC), NHS containing C5 inhibitor, or depleted for terminal complement components C5, C7 or C9 in the presence of 50 nM of the potential-sensitive dye $DiOC_6$ (excitation wavelength, 484 nm; emission wavelength, 501 nm). Fluorescence was measured by flow cytometry. Cells were also treated with the intracellular Ca^{2+} chelator BAPTA-AM. (**A**) BAPTA-AM treatment resulted in a decrease in potential, indicating the disruption of the mitochondrial membrane. Data are means±s.d. of three independent experiments. (**B**) The membrane-permeant JC-1 dye was also used in order to monitor changes in mitochondrial membrane potential. Cells were loaded with the ratiometric mitochondrial potential indicator JC-1 at 5 μM for 30 minutes at 37℃. Cells were then treated with either HI-NHS or anti-CD59 and NHS in order to investigate whether MAC will depolarise the mitochondrial membrane. Images were taken before addition of the treatment (0 min), and at 10 min and 30 min following stimulation. The cells were illuminated at 488 nm and the emission was collected between 515/545 nm and 575/625 nm. Regions of high mitochondrial polarization are indicated by red fluorescence due to J-aggregate formation by the concentrated dye. Depolarised regions are indicated by the green fluorescence of the JC-1 monomers. (**C**) Cell extracts were also collected and subjected to subcellular fractionation. Cytochrome *c* (cyt C) was detected in the cytosolic fraction using western blotting and an anti-cytochrome *c* antibody.

microscopy. In cells treated with HI-NHS, NLRP3 was localised in the cytoplasm (Fig. 6G, top row), there was no co-localisation with the mitochondrial marker MitoTracker. This was confirmed by the statistical analysis, which showed an *R*(obs) of 0.086, indicating that there was no significant correlation between NLRP3 and the mitochondria. This localisation changed dramatically after MAC-induced NLRP3 activation. NLRP3 relocated into the perinuclear space and co-localised with structures that stained positive for mitochondria (Fig. 6G, middle row). Statistical analysis revealed an *R*(obs) of 0.928, which suggests strong co-localisation. In cells which were incubated with NHS depleted of C5 or HI-NHS, NLRP3 did not co-localise with mitochondria demonstrating a dependence upon MAC formation. Similar results were observed in cells incubated with anti-CD59 and NHS in the presence of BAPTA (Fig. 6G, bottom row), confirming the Ca^{2+}-dependence of the mechanism of activation. Taken together, our results support a model in which Ca^{2+} signalling critically regulates MAC-induced NLRP3 inflammasome activation by triggering mitochondrial damage.

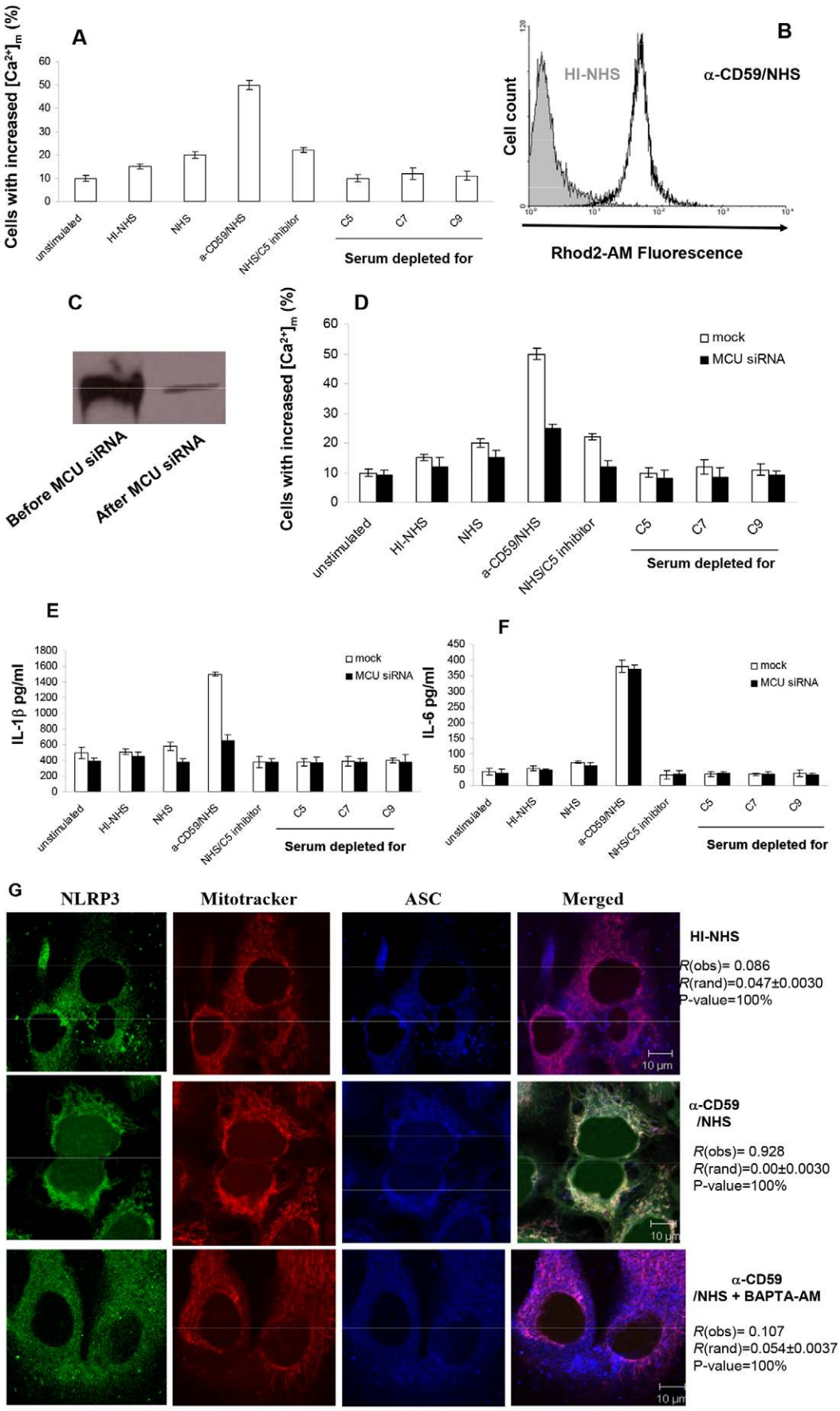

Fig. 6. See next page for legend.

Discussion

The complement system is an essential part of the innate immune system, involved in eliminating pathogens. However, inappropriate or excessive complement activation is also involved in a large number of inflammatory, neurodegenerative, ischemic and age-related diseases. Although it can be activated by three distinct pathways, all pathways converge to the terminal complement pathway. Triggering this final pathway can lead to either lytic or sublytic activation. Lytic activation results in the formation of a transmembrane channel, causing osmotic lysis of the target cell. Although complement was first recognised for its "classical" capacity to lyse cells, it has become apparent that "sublytic" deposition of MAC can also occur. The diameter of the pore created varies according to the number of C9 molecules that are available to complex with C5b-8. Pore size, numbers of pores and capacity of cells to remove MAC all influence whether the target cell is lysed. Deposition of sublytic amounts of MAC triggers signalling and can have a wide range of effects on the target cell such as secretion, adherence, aggregation, chemotaxis, cell division, etc. Ca^{2+} influx has been shown to be one of the consequences of MAC-induced activation, resulting in Ca^{2+} oscillations that can last up to 45 min (Nicholson-Weller and Halperin, 1993) and seem to determine the fate of a cell attacked by complement.

In this study we set out to investigate the non-lytic effects of complement on nucleated cells and whether these non-lytic effects extend to the activation of the inflammasome. The inflammasomes are key cytosolic innate immune sensors which detect cellular stress in a variety of infectious and "sterile" settings, triggering the induction of critical inflammatory pathways. Our results demonstrated that sublytic concentrations of MAC were able to trigger inflammasome activation. In particular, NLRP3 was shown to be activated in response to sublytic MAC, leading to caspase 1 activation and IL-1β production.

The NLRP3 inflammasome is a cytoplasmic complex consisting of the regulatory subunit NALP3, the adaptor ASC and the effector subunit caspase-1. It has been shown that NALP3 can be activated by a wide variety of molecules suggesting that it probably does not directly bind to its known activators, but is activated by an indirect mechanism. It is believed that inflammasomes require a two-step method of activation. The first or priming signal can be triggered from a transcriptionally active PRR or cytokine receptor, this leads to transcriptional activation of the genes encoding pro-IL-1b and pro-IL-18 (Bauernfeind et al., 2009). The prevailing view is that the second signal is believed to be triggered in response to various stress signals associated with damaged self (Martinon et al., 2009). Four distinct mechanisms have been proposed for NLRP3 activation: 1) potassium efflux (Kanneganti et al., 2007), 2) generation of reactive oxygen species (ROS) (Dostert et al., 2008), 3) lysosomal disruption and most recently (Halle et al., 2008; Hornung et al., 2008) 4) Ca^{2+} influx (Feldmeyer et al., 2007; Murakami et al., 2012; Lee et al., 2012). The question that arises is how is IL-1β triggered in response to sublytic MAC and what is the mechanism of MAC-induced NALP3 activation?

Our data demonstrate that MAC-induced Ca^{2+} efflux triggers NALP3 activation. Intracellular Ca^{2+} signalling has been shown to be important in NALP3 activation in response to a wide range of stimuli (Murakami et al., 2012; Lee et al., 2012), including UV irradiation (Feldmeyer et al., 2007), suggesting that it is a common mechanism of NALP3 activation irrespective of the trigger. Sublytic MAC activation is due to the transient insertion of MAC into the membrane, generating pores that allow the influx of ions such as Ca^{2+} and Na^{+}, increasing the cytosolic Ca^{2+} concentration. These rises in intracellular Ca^{2+} occur both via the pore and through release from stores (Morgan and Campbell, 1985). This is in agreement with our data that suggest that this increased cytosolic Ca^{2+} concentration is at least partly due to Ca^{2+} release from the ER lumen via RyR and IP_3R channels. These channels seem to facilitate the accumulation of Ca^{2+} into the mitochondrial matrix.

Mitochondria have long been known to be far more than passive Ca^{2+} sinks. The central role of mitochondrial Ca^{2+} transport mechanisms is to respond to physiological Ca^{2+} in the cytosol in order to take up Ca^{2+} for regulating energy production. Thus, the balance between Ca^{2+} influx and efflux across the mitochondrial inner membrane is crucial for establishing Ca^{2+} homeostasis within the cell and thus special Ca^{2+} transport mechanisms exist, one of which is the newly identified MCU. The physiological increase of mitochondrial Ca^{2+} serves as a key signal for regulating mitochondrial activity. However, non-physiological mitochondrial Ca^{2+} overload depolarises the membrane. In the case of sublytic MAC, calcium seems to play a key role in determining the fate of the target cell. The increased cytosolic Ca^{2+} seems to be transported via MCU into the inner mitochondrial membrane causing overload and depolarization of the membrane.

We then examined whether this loss in Ca^{2+} homeostasis is also able to induce apoptosis, as it has been suggested previously that MAC may play an important role in regulating apoptosis (Morgan, 1989; Soane et al., 1999; Niculescu et al., 2003). To do this we looked at the effect of sublytic MAC on mitochondrial dysfunction, particularly $\Delta\psi_m$ as well as cytochrome *c* efflux into the cytosol. After sublytic MAC deposition we found a drop in $\Delta\psi_m$ was accompanied by cytochrome *c* efflux into the cytosol. In addition, Ca^{2+} was taken up into the mitochondria and NLRP3 was found to relocate from the cytoplasm to the mitochondria in response to MAC activation, which is in agreement with Zhou et al. who have shown that upon inflammasome activation, NALP3 co-localises with the mitochondria (Zhou et al., 2011). Our data suggests that Ca^{2+} signalling critically regulates MAC-

Fig. 6. Sublytic MAC-induced mitochondrial Ca^{2+} uptake. (**A**) Lung epithelial cells were incubated with HI-NHS, NHS, anti-CD59 and 5% NHS (in order to provoke <5% cell death – sublytic MAC), NHS containing C5 inhibitor, or depleted for terminal complement components C5, C7 or C9, in the presence of Rhod2 AM then analysed by flow cytometry. (**B**) Representative flow cytometry histogram after Rhod2 AM staining of cells treated with HI-NHS (grey histogram) or anti-CD59 and NHS (white histogram). MCU expression was knocked down by siRNA (**C**) and the cells were again incubated with HI-NHS, NHS, anti-CD59 and 5% NHS (in order to provoke <5% cell death – sublytic MAC), NHS containing C5 inhibitor or depleted for terminal complement components C5, C7 or C9 in the presence of Rhod2-AM then analysed by flow cytometry (**D**). Supernatant was also collected after 12 hours and analysed for IL-1β (**E**) and IL-6 (**F**) using the CBA system. The data represent the mean±s.d. of three independent experiments. The co-localisation of the NLRP3 inflammasome components with mitochondria in response to sub-lytic MAC attack was also investigated using confocal microscopy (**G**). Cells were stimulated with either HI-NHS or anti-CD59 and NHS for 1 h and subsequently fixed. NLRP3 was stained using a rabbit anti-NLRP3 Fab conjugated to Alexa 4886, mitochondria were stained using Mitotracker and ASC was stained using a goat anti-ASC Fab conjugated to Alexa 633. Cells were imaged using a Zeiss 510 confocal microscope. Scale bars: 10 μm. The data represent the means of three independent experiments. Co-localisation coefficients [*R*(obs)] were calculated using Costes' approach.

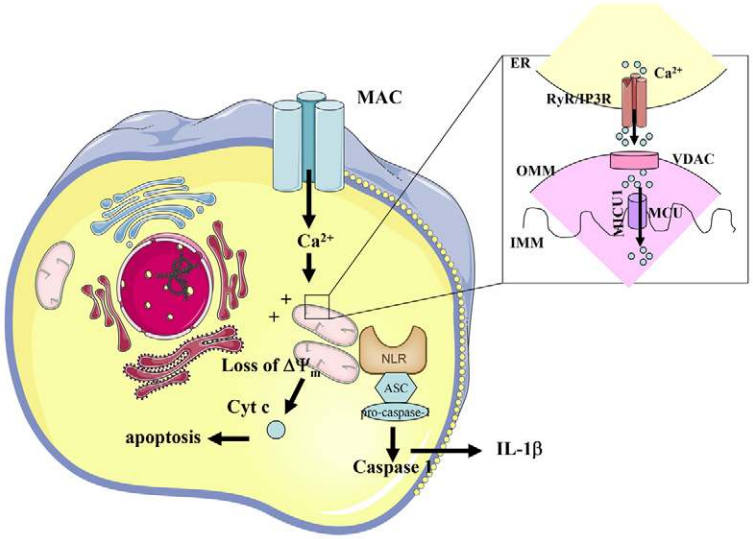

Fig. 7. Proposed model of sublytic MAC-induced-NLRP3 inflammasome activation. Formation of MAC results in the influx of Ca^{2+}. This in turn causes Ca^{2+}release from the ER via RyR/IP3IR channels. Ca^{2+} uptake in the inner mitochondrial membrane occurs via MCU, leading to loss of mitochondrial transmembrane potential ($\Delta\Psi$m). NLRP3 senses the increase in Ca^{2+} as well as the mitochondrial dysfunction, triggering caspase 1 activation and IL-1β secretion; in parallel, there is cytochrome *c* release and activation of the apoptosome.

induced NLRP3 inflammasome activation by triggering mitochondrial damage. This is in agreement with previous studies where it was suggested that following MAC attack, the ensuing cell crisis is centred on the mitochondrion (Papadimitriou et al., 1994). Our data suggests a model where, following sublytic MAC attack, excess Ca^{2+} results in mitochondrial overload, loss of mitochondrial transmembrane potential, resulting in an energy crisis within the cells as energy consuming ion pumps try to bring back Ca^{2+} homeostasis, which in turn triggers NLPR3 inflammasome activation, IL-1β secretion, cytochrome *c* release into the cytoplasm and caspase activation ultimately leading to apoptosis (Fig. 7). This suggests a potential role for the NALP3 inflammasome in "sensing" dyregulated Ca^{2+} homeostasis and inducing inflammation in the chronic inflammatory, neurodegenerative and infectious diseases caused by MAC, such as rheumatoid arthritis, dense deposit disease, Alzheimer's disease, multiple sclerosis, sepsis and even atherosclerosis. Our study demonstrates for the first time the mechanism by which sublytic MAC attack can activate the production of inflammatory mediators and amplify an ongoing inflammatory response by triggering inflammasome activation.

Materials and Methods

Cells

Primary human lung epithelial cells were obtained from TCS Cell Works (Buckingham, UK). They were passaged and maintained in the epithelial cell medium provided by TCS.

Chemicals/reagents

All chemicals were obtained from Sigma (UK). FLUO4-AM and BAPTA-AM were purchased from Molecular Probes (Life Technologies, Paisley, UK). Rabbit polyclonal caspase 1 p10 antibody, rabbit polyclonal NLRP3 antibody, rabbit polyclonal NLRP1 antibody, goat polyclonal NLRC4 antibody and ASC goat polyclonal antibody were purchased from Santa Cruz Biotechnology Ltd (CA, USA). The C5 inhibitor OmCI, as well as rabbit polyclonal anti-human CD59 antiserum, was raised in house (Prof. B.P. Morgan, Cardiff University).

Complement attack and MAC deposition assay

Confluent lung epithelial cells were serum-starved for 2 days, and incubated with heat-treated rabbit polyclonal anti-human CD59 antiserum for 1 h at 37℃. Antibody-sensitised cells were washed and exposed to NHS, C5 inhibitor OmCI-treated NHS, HI-NHS (10 min at 56℃), or NHS that was immunoaffinity depleted for C5, C7, or C9 as a complement deficient control, at 37℃ for another hour. Afterwards, the cells were washed thoroughly and incubated with serum-free medium. The amount of NHS selected for the MAC deposition assay was defined by calibration using the propidium iodide (PI) viability assay, where sublytic doses of MAC were characterised as <5% cell death. MAC formation was verified by flow cytometry using anti-C9 neoantigen-specific monoclonal antibody B7.

RNA interference

RNA interference was used in order to silence the NLRP1, NLRP3, NLRC4 and ASC genes. Different pshRNA clones were generated using the psh7SK vector from Invitrogen against the sequence: for NLRP1, GAAGGAGGAGCTGAAG-GAGTT and GGCCTGATTATGTGGAGGAGA, for NLRP3 GGAAGTGGA-CTGCGAGAAGTT, for NLRC4, GGATGCTGCTAGAGGGATCAT and GACA-ACTGGGCTCCTCTGTAA, and for ASC AACTG GACCTGCAAGGACTTG. To silence MCU specific siRNA were utilised as described (De Stefani et al., 2011).

Lung epithelial cells (1×10^5) were seeded in six-well plates and transfected with 0.5 μg of pshRNA for either NLRP1, NLRP3, NLRC4 or scrambled shRNA as a control using Lipofectamine 2000 (Invitrogen, Paisley, UK). After 48 h the level of silencing was determined by western blotting in cell lysates. Transfections with the specific shRNAs resulted in an ~85% decrease in receptor expression as determined by western blotting whereas transfection of cells with the scrambled siRNA did not show any decrease in the specific gene expression.

Cytokine assays

At intervals after sublytic MAC deposition, the serum-free medium was harvested and frozen until the assays were performed. The Becton Dickinson (Oxford, UK) Cytometric bead array (CBA) system was used in order to determine IL-1β and IL-6 level.

Cytosolic calcium measurement

The calcium-sensitive dye FLUO4-AM (excitation wavelength, 506 nm; emission wavelength, 526 nm) was used to measure the cytosolic calcium level. Intracellular esterases cleave the AM group leaving the membrane impermeable FLUO4 trapped in the cell. FLUO4 is almost non-fluorescent unless it is bound to calcium, and its fluorescence increases with rising calcium concentration. Cells were incubated in DMEM supplemented with 10% FBS and 1 mM FLUO4-AM, at 37℃, for 1 h before MAC deposition. At various times post-attack as described above, cells were harvested, pelleted, and resuspended in ice-cold PBS containing 10 mM glucose and 10% FBS. Cytosolic calcium levels were determined by flow cytometry.

Measurement of mitochondrial membrane potential (Δψm)

In order to measure the mitochondrial transmembrane potential (Δψm) cells (4×10^5) were stained with 50 nM of the potential-sensitive dye $DiOC_6(3)$ (excitation wavelength, 484 nm; emission wavelength, 501 nm) for 5 min at 37℃. Fluorescence was measured by flow cytometry. A drop in $DiOC_6(3)$ staining indicates the disruption of the mitochondrial potential.

The membrane-permeant JC-1 dye was used in order to monitor changes in mitochondrial membrane potential. JC-1 dye exhibits potential-dependent accumulation in mitochondria, indicated by a fluorescence emission shift from green (~529 nm) to red (~590 nm). Cells were loaded with the ratiometric mitochondrial potential indicator JC-1 at 5 μM for 30 minutes at 37℃. Cells were then treated with either HI-NHS or anti-CD59 and NHS in order to investigate whether MAC will depolarise the mitochondrial membrane. Images were taken before addition of the treatment (0 min), as well as at 10 min and 30 min

following stimulation. The cells were illuminated at 488 nm and the emission was collected between 515/545 nm and 575/625 nm.

Mitochondrial calcium measurement

Rhod2 AM (excitation wavelength, 552 nm; emission wavelength, 581 nm) was used in order to measure the mitochondrial calcium level. The fluorescent dye Rhod2 AM has a net positive charge, facilitating its sequestration into mitochondria through membrane potential-driven uptake. The AM ester of the probe is cell permeable and rapidly cleaved in the mitochondria to yield the Rhod2 indicator, which displays a large increase in fluorescence intensity upon binding Ca^{2+} (Trollinger et al., 1997). Cells (4×10^5) were incubated with HI-NHS, NHS, anti-CD59 and 5% NHS (in order to provoke <5% cell death – sublytic MAC), with or without C5 inhibitor, or serum depleted for terminal complement components C5, C7 or C9. Following stimulation, the cells were harvested, pelleted and resuspended in ice-cold PBS containing 10 mM glucose, 10% FCS and 10 µM Rhod2 AM. Mitochondrial calcium levels were determined by flow cytometry.

Subcellular fractionation

The subcellular proteome extraction kit (Calbiochem, UK) was used to isolate the cytosolic fraction of cells according to the manufacturer's instructions. Briefly, cells (5×10^6) were harvested, pelleted, washed twice in PBS, resuspended in ice-cold extraction I buffer containing protease inhibitor mixture and incubated for 10 min at 4℃. The suspension was centrifuged at 1,200×g at 4℃ for 10 min. The supernatant was used as the cytosolic fraction.

Confocal microscopy

Human primary epithelial cells on microchamber Lab-tek culture slides (Life Technologies, Paisley, UK), were incubated with HI-NHS, or anti-CD59 and 5% NHS (in order to provoke <5% cell death – sublytic MAC) and controls as above. Cells were rinsed twice in PBS/0.02% BSA, prior to fixation with 4% formaldehyde for 15 min. The cells were fixed in order to prevent potential re-organisation of the proteins during the course of the experiment. Cells were permeabilised using PBS/0.02% BSA/0.02% Saponin and labelled with antibodies for NLRP3, caspase p10, and ASC directly labelled with the appropriate fluorophore. Alternatively, human primary epithelial cells on microchamber culture slides, were incubated with HI-NHS, or anti-CD59 and 5% NHS (in order to provoke <5% cell death – sublytic MAC) and controls as above and subsequently incubated with MitoTracker prior to fixation with 4% formaldehyde for 15 min and labelled as described above.

Cells were imaged on a Carl Zeiss, Inc. LSM510 META confocal microscope (with an Axiovert 200 fluorescent microscope) using a 1.4 NA 63×Zeiss objective. The images were analysed using LSM 2.5 image analysis software (Carl Zeiss, Inc.).

In order to quantify the degree of co-localisation, we used Costes' approach. Costes' approach, Pearson's correlation coefficients and *P* values were calculated using MBF ImageJ with JACoP (Just Another Colocalisation Plugin; http://macbiophotonics.ca/).

Author contributions

Conception and design: K.T., M.T., B.P.M. Acquisition of data, or analysis and interpretation of data: K.T., T.R.H., M.T., B.P.M. Drafting the article or revising it critically for important intellectual content: K.T., T.R.H., M.T., B.P.M. Provision of reagents: T.R.H., B.P.M.

Funding

This research received no specific grant from any funding agency in the public, commercial or not-for-profit sectors.

References

Bauernfeind, F. G., Horvath, G., Stutz, A., Alnemri, E. S., MacDonald, K., Speert, D., Fernandes-Alnemri, T., Wu, J., Monks, B. G., Fitzgerald, K. A. et al. (2009). Cutting edge: NF-kappaB activating pattern recognition and cytokine receptors license NLRP3 inflammasome activation by regulating NLRP3 expression. *J. Immunol.* **183**, 787-791.

Baughman, J. M., Perocchi, F., Girgis, H. S., Plovanich, M., Belcher-Timme, C. A., Sancak, Y., Bao, X. R., Strittmatter, L., Goldberger, O., Bogorad, R. L. et al. (2011). Integrative genomics identifies MCU as an essential component of the mitochondrial calcium uniporter. *Nature* **476**, 341-345.

Bhakdi, S. and Tranum-Jensen, J. (1991). Complement lysis: a hole is a hole. *Immunol. Today* **12**, 318-320, discussion 321.

Bolte, S. and Cordelières, F. P. (2006). A guided tour into subcellular colocalization analysis in light microscopy. *J. Microsc.* **224**, 213-232.

Celsi, F., Pizzo, P., Brini, M., Leo, S., Fotino, C., Pinton, P. and Rizzuto, R. (2009). Mitochondria, calcium and cell death: a deadly triad in neurodegeneration. *Biochim. Biophys. Acta* **1787**, 335-344.

De Stefani, D., Raffaello, A., Teardo, E., Szabò, I. and Rizzuto, R. (2011). A forty-kilodalton protein of the inner membrane is the mitochondrial calcium uniporter. *Nature* **476**, 336-340.

Deniaud, A., Sharaf el dein, O., Maillier, E., Poncet, D., Kroemer, G., Lemaire, C. and Brenner, C. (2008). Endoplasmic reticulum stress induces calcium-dependent permeability transition, mitochondrial outer membrane permeabilization and apoptosis. *Oncogene* **27**, 285-299.

Dostert, C., Pétrilli, V., Van Bruggen, R., Steele, C., Mossman, B. T. and Tschopp, J. (2008). Innate immune activation through Nalp3 inflammasome sensing of asbestos and silica. *Science* **320**, 674-677.

Fang, C., Zhang, X., Miwa, T. and Song, W. C. (2009). Complement promotes the development of inflammatory T-helper 17 cells through synergistic interaction with Toll-like receptor signaling and interleukin-6 production. *Blood* **114**, 1005-1015.

Feldmeyer, L., Keller, M., Niklaus, G., Hohl, D., Werner, S. and Beer, H. D. (2007). The inflammasome mediates UVB-induced activation and secretion of interleukin-1beta by keratinocytes. *Curr. Biol.* **17**, 1140-1145.

Hajishengallis, G. and Lambris, J. D. (2010). Crosstalk pathways between Toll-like receptors and the complement system. *Trends Immunol.* **31**, 154-163.

Hajishengallis, G. and Lambris, J. D. (2011). Microbial manipulation of receptor crosstalk in innate immunity. *Nat. Rev. Immunol.* **11**, 187-200.

Halle, A., Hornung, V., Petzold, G. C., Stewart, C. R., Monks, B. G., Reinheckel, T., Fitzgerald, K. A., Latz, E., Moore, K. J. and Golenbock, D. T. (2008). The NALP3 inflammasome is involved in the innate immune response to amyloid-beta. *Nat. Immunol.* **9**, 857-865.

Hawlisch, H., Belkaid, Y., Baelder, R., Hildeman, D., Gerard, C. and Köhl, J. (2005). C5a negatively regulates toll-like receptor 4-induced immune responses. *Immunity* **22**, 415-426.

Hornung, V., Bauernfeind, F., Halle, A., Samstad, E. O., Kono, H., Rock, K. L., Fitzgerald, K. A. and Latz, E. (2008). Silica crystals and aluminum salts activate the NALP3 inflammasome through phagosomal destabilization. *Nat. Immunol.* **9**, 847-856.

Ichinohe, T., Pang, I. K. and Iwasaki, A. (2010). Influenza virus activates inflammasomes via its intracellular M2 ion channel. *Nat. Immunol.* **11**, 404-410.

Kanneganti, T. D., Lamkanfi, M., Kim, Y.-G., Chen, G., Park, J.-H., Franchi, L. and Vandenabeele, P. (2007). Pannexin-1-mediated recognition of bacterial molecules activates the cryopyrin inflammasome independent of Toll-like receptor signaling. *Immunity* **26**, 433-443.

Lee, G. S., Subramanian, N., Kim, A. I., Aksentijevich, I., Goldbach-Mansky, R., Sacks, D. B., Germain, R. N., Kastner, D. L. and Chae, J. J. (2012). The calcium-sensing receptor regulates the NLRP3 inflammasome through Ca2+ and cAMP. *Nature* **492**, 123-127.

Martinon, F., Mayor, A. and Tschopp, J. (2009). The inflammasomes: guardians of the body. *Annu. Rev. Immunol.* **27**, 229-265.

Mayer, M. M. (1972). Mechanism of cytolysis by complement. *Proc. Natl. Acad. Sci. USA* **69**, 2954-2958.

Morgan, B. P. (1989). Complement membrane attack on nucleated cells: resistance, recovery and non-lethal effects. *Biochem. J.* **264**, 1-14.

Morgan, B. P. and Campbell, A. K. (1985). The recovery of human polymorphonuclear leucocytes from sublytic complement attack is mediated by changes in intracellular free calcium. *Biochem. J.* **231**, 205-208.

Morgan, B. P., Luzio, J. P. and Campbell, A. K. (1986). Intracellular Ca2+ and cell injury: a paradoxical role of Ca2+ in complement membrane attack. *Cell Calcium* **7**, 399-411.

Murakami, T., Ockinger, J., Yu, J., Byles, V., McColl, A., Hofer, A. M. and Horng, T. (2012). Critical role for calcium mobilization in activation of the NLRP3 inflammasome. *Proc. Natl. Acad. Sci. USA* **109**, 11282-11287.

Nicholson-Weller, A. and Halperin, J. A. (1993). Membrane signaling by complement C5b-9, the membrane attack complex. *Immunol. Res.* **12**, 244-257.

Niculescu, T., Weerth, S., Soane, L., Niculescu, F., Rus, V., Raine, C. S., Shin, M. L. and Rus, H. (2003). Effects of membrane attack complex of complement on apoptosis in experimental autoimmune encephalomyelitis. *Ann. New York Acad. Sci.* **1010**, 530-533.

Papadimitriou, J. C., Phelps, P. C., Shin, M. L., Smith, M. W. and Trump, B. F. (1994). Effects of Ca2+ deregulation on mitochondrial membrane potential and cell viability in nucleated cells following lytic complement attack. *Cell Calcium* **15**, 217-227.

Rathinam, V. A., Vanaja, S. K. and Fitzgerald, K. A. (2012). Regulation of inflammasome signaling. *Nat. Immunol.* **13**, 333-2.

Smiley, S. T., Reers, M., Mottola-Hartshorn, C., Lin, M., Chen, A., Smith, T. W., Steele, G. D., Jr and Chen, L. B. (1991). Intracellular heterogeneity in mitochondrial membrane potentials revealed by a J-aggregate-forming lipophilic cation JC-1. *Proc. Natl. Acad. Sci. USA* **88**, 3671-3675.

Soane, L., Rus, H., Niculescu, F. and Shin, M. L. (1999). Inhibition of oligodendrocyte apoptosis by sublytic C5b-9 is associated with enhanced synthesis of bcl-2 and mediated by inhibition of caspase-3 activation. *J. Immunol.* **163**, 6132-6138.

Trollinger, D. R., Cascio, W. E. and Lemasters, J. J. (1997). Selective loading of Rhod 2 into mitochondria shows mitochondrial Ca2+ transients during the contractile cycle in adult rabbit cardiac myocytes. *Biochem. Biophys. Res. Commun.* **236**, 738-742.

Wang, M., Krauss, J. L., Domon, H., Hosur, K. B., Liang, S., Magotti, P., Triantafilou, M., Triantafilou, K., Lambris, J. D. and Hajishengallis, G. (2010). Microbial hijacking of complement-toll-like receptor crosstalk. *Sci. Signal.* **3**, ra11.

Zhang, X., Kimura, Y., Fang, C., Zhou, L., Sfyroera, G., Lambris, J. D., Wetsel, R. A., Miwa, T. and Song, W. C. (2007). Regulation of Toll-like receptor-mediated inflammatory response by complement in vivo. *Blood* **110**, 228-236.

Zhou, R., Yazdi, A. S., Menu, P. and Tschopp, J. (2011). A role for mitochondria in NLRP3 inflammasome activation. *Nature* **469**, 221-225.